Academic Journal of Applied Sciences
ISSN: 3105-0549 (Print), ISSN: 3105-0557 (Online) | Vol. 2, No. 1, 2026

Lamb Waves in One-Dimensional Hexagonal Piezoelectric Quasicrystal Layered Plates

Zhenquan He *

Institute of Mechanical Monitoring and Fault Diagnosis & Henan International Joint Laboratory of Advanced Electronic Packaging Materials Precision Forming, Henan Polytechnic University, Jiaozuo 454000, P.R. China

* **Corresponding author**: (Email: 15039442176@163.com)

Abstract: Lamb wave propagation in one-dimensional hexagonal piezoelectric quasicrystal (PQC) layered plates is investigated. The coupled phonon, phason, and electric fields are considered simultaneously, and a multilayered plate model with traction-free and electrically open-circuited surfaces is established. By introducing rectangular window functions and expanding the field variables in each layer using Legendre polynomials, the governing wave equations are transformed into a matrix eigenvalue problem, from which the phase velocity dispersion characteristics are obtained. The effects of phonon–phason coupling, layer thickness, stacking sequence, and piezoelectric properties on Lamb wave behavior are systematically examined. The results show that the stacking sequence and layer thickness have a pronounced and mode-dependent influence on the dispersion curves, indicating that guided-wave characteristics can be effectively tailored through structural design. Moreover, the piezoelectric effect increases the phase velocities of both phonon and phason modes, while an increase in the dielectric constant weakens this effect. The dielectric constant of the middle layer plays a dominant role at low frequencies, whereas that of the surface layer becomes more influential at high frequencies. These findings provide theoretical guidance for the design of multifunctional PQC layered structures with controllable wave characteristics.

Keywords: Piezoelectric quasicrystal, Lamb wave, Layered composite plate, Dispersion, Legendre polynomial expansion, Phonon–phason coupling.

1. Introduction

Piezoelectric quasicrystal (PQC) materials combine the aperiodic long-range ordered structure of quasicrystals with the electromechanical coupling characteristics of piezoelectric media, exhibiting remarkable mechanical, electrical, and wave propagation properties [1, 2]. Compared with conventional piezoelectric crystals, PQC materials possess additional phason degrees of freedom beyond the conventional phonon field, leading to more complex multiphysical coupling. Owing to these unique characteristics, PQC materials have shown considerable potential in advanced functional devices and smart structural systems, such as acoustic wave manipulation, ultrasonic transducers, intelligent sensing, energy conversion, and structural health monitoring [3-5]. In practical engineering applications, layered structures are widely adopted because they provide greater flexibility to tailor material performance through stacking-sequence design, thickness variation, and material combinations [6]. Consequently, PQC layered structures have attracted increasing attention as promising multifunctional composites with tunable wave characteristics and enhanced electromechanical performance. Therefore, investigating wave propagation in PQC layered plates is of both theoretical significance and engineering importance.

Among various guided waves in plate-like structures, Lamb waves have been extensively studied due to their dispersive and multimodal characteristics, as well as their high sensitivity to structural discontinuities and material inhomogeneity [7]. Over the past decades, Lamb wave propagation in elastic and piezoelectric layered plates has been widely investigated in the context of nondestructive evaluation, damage detection, and wave control. Existing studies have demonstrated that the propagation characteristics of Lamb waves can be effectively manipulated by changing material anisotropy, thickness distribution, and electrical boundary conditions. In conventional piezoelectric layered structures, the electromechanical coupling effect significantly influences phase velocity dispersion, modal characteristics, and energy transmission behavior [8-10]. These findings provide an important theoretical foundation for the development of wave-based smart structures and functional composites.

The discovery of quasicrystals by Shechtman et al. [11] fundamentally extended the framework of classical solid mechanics. Unlike periodic crystals, quasicrystals possess long-range orientational order without translational periodicity and exhibit additional phason fields associated with atomic rearrangement. To describe these unique characteristics, generalized elasticity theories incorporating phonon–phason coupling were established by Lubensky et al. [12] and Bak [13]. Based on these theories, extensive investigations have been conducted on the static and dynamic behaviors of quasicrystal materials [14-16]. Previous studies revealed that the phonon–phason coupling effect can significantly modify wave dispersion behavior, generate additional wave modes, and alter energy transport mechanisms [17]. More recently, wave propagation in quasicrystal plates, functionally graded structures, and piezoelectric quasicrystal media has gradually become an active research topic.

Despite these developments, studies on Lamb waves in PQC layered plates remain very limited. Most existing investigations mainly focus on single-layered or functionally graded quasicrystal structures [18-20], while the effects of structural heterogeneity introduced by multilayered configurations have not been systematically clarified. In particular, the combined influences of phonon–phason

coupling, piezoelectric effect, layer thickness variation, and stacking sequence on guided wave propagation are still not fully understood. Therefore, it is necessary to develop stable and efficient theoretical formulations for analyzing wave propagation in PQC layered structures.

Motivated by the above considerations, the present study investigates Lamb wave propagation in one-dimensional hexagonal PQC layered plates. Based on the generalized theory of piezoelectric quasicrystals, the governing equations involving phonon, phason, and electric fields are established simultaneously. By introducing Legendre polynomial expansions, the wave problem is transformed into a matrix eigenvalue formulation, which provides an efficient and numerically stable approach for solving the dispersion characteristics of PQC layered plates. The effects of layer thickness, stacking sequence, and piezoelectric properties on the propagation characteristics of Lamb waves are systematically analyzed. The results obtained provide useful theoretical guidance for the design and optimization of PQC-based acoustic filters, waveguides, sensors, and adaptive layered composite components.

2. Mathematics and Formulation

We consider a horizontally infinite N-layered PQC plate with a total thickness of hN, as shown in Figure 1. The horizontal plane (x, y) is located at its upper surface, and the layered structure is arranged in the positive z-direction. Lamb waves propagate along the x-direction. The quasi-periodic direction is along the z-direction.

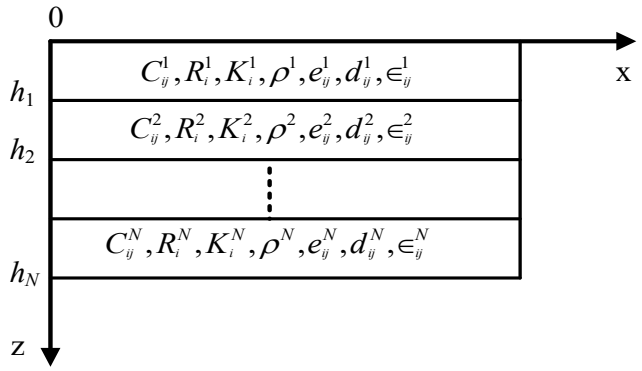

Figure 1. Schematic diagram of an infinite N-layered PQC plate

Based on the Bak model and neglecting body forces and external electric fields, the dynamic equations for the PQC layered plate are written as follows [18]:

$$\begin{aligned}
&\frac{\partial T_{xx}}{\partial x}+\frac{\partial T_{xz}}{\partial z}=\rho\ddot{u}_x\\
&\frac{\partial T_{xz}}{\partial x}+\frac{\partial T_{zz}}{\partial z}=\rho\ddot{u}_z\\
&\frac{\partial H_{xz}}{\partial x}+\frac{\partial H_{zz}}{\partial z}=\rho\ddot{w}_z\\
&\frac{\partial D_x}{\partial x}+\frac{\partial D_z}{\partial z}=0
\end{aligned} \tag{1}$$

Where ρ is the material density. u_i and w_i represent the displacements in the phonon and phason fields, respectively. T_{ij} and H_{ij} are stresses in the phonon and phason fields, respectively. Di is the electric displacement.

The generalized relations between strains and displacements, electric field strength, and electric potential are expressed as follows [19]:

$$\begin{aligned}
&\varepsilon_{xx}=\frac{\partial u_x}{\partial x},\varepsilon_{zz}=\frac{\partial u_z}{\partial z},\varepsilon_{xz}=\frac{1}{2}\left(\frac{\partial u_x}{\partial z}+\frac{\partial u_z}{\partial x}\right),\\
&w_{zx}=\frac{\partial w_z}{\partial x},w_{zz}=\frac{\partial w_z}{\partial z},E_x=-\frac{\partial\phi}{\partial x},E_z=-\frac{\partial\phi}{\partial z},
\end{aligned} \tag{2}$$

Where ε_{ij} and w_{ij} represent the strains in the phonon and phason fields, respectively. E_i is the electric field strength, and ϕ is the electric potential.

For layered PQC plates, the traction-free and electrically open-circuited boundary conditions are assumed at the top and bottom surfaces, which means the phonon and phason tractions, as well as the normal electric displacement, vanish at the top and bottom surfaces ($T_{zz}=T_{xz}=T_{yz}=H_{zz}=H_{zx}=H_{zy}=D_z=0$). Furthermore, the displacements and stresses are continuous at the interlayer interfaces.

To address the traction-free and open-circuited boundary conditions, a rectangular window function consisting of Heaviside step functions is introduced.

$$I_{h_0,h_N}(z)=Heaviside[h_0]-Heaviside[h_N]=\begin{cases}1, h_0\le z\le h_N\\ 0, elsewhere\end{cases} \tag{3}$$

Where $h_0=0$.

In this way, the boundary conditions are automatically embedded into the constitutive equations, leading to the following constitutive equations for a PQC layered plate. Since both the quasi-periodic direction and the polarization direction are along the z-axis, the phason displacement components in the x and y directions are zero, while the phason displacement component in the z direction is non-zero. The constitutive relations are written as follows:

$$\begin{aligned}
T_{xx}&=\left(C_{11}\varepsilon_{xx}+C_{12}\varepsilon_{yy}+C_{13}\varepsilon_{zz}+R_1w_{zz}-e_{31}E_z\right)I_{0,h_N}(z)\\
T_{zz}&=\left(C_{13}\varepsilon_{xx}+C_{13}\varepsilon_{yy}+C_{33}\varepsilon_{zz}+R_2w_{zz}-e_{33}E_z\right)I_{0,h_N}(z)\\
T_{xz}&=\left(2C_{55}\varepsilon_{xz}+R_3w_{zx}-e_{15}E_x\right)I_{0,h_N}(z)
\end{aligned} \tag{4a}$$

$$H_{zz} = \left(R_1\varepsilon_{xx} + R_1\varepsilon_{yy} + R_2\varepsilon_{zz} + K_1 w_{zz} - d_{33}E_z\right) I_{0,h_N}(z)$$
$$H_{zx} = \left(2R_3\varepsilon_{xz} + K_2 w_{zx} - d_{15}E_x\right) I_{0,h_N}(z) \tag{4b}$$

$$D_z = \left[e_{31}\left(\varepsilon_{xx} + \varepsilon_{yy}\right) + e_{33}\varepsilon_{zz} + d_{33}w_{zz} + \in_{33} E_z\right] I_{0,h_N}(z)$$
$$D_x = \left[2e_{15}\varepsilon_{zx} + d_{15}w_{zx} + \in_{11} E_x\right] I_{0,h_N}(z) \tag{4c}$$

Where C_{ij}, K_i, R_i are the elastic parameters in the phonon and phason fields, and the phonon-phason coupling coefficients. $e_{ij}, d_{ij}, \in_{ij}$ denote the piezoelectric and dielectric coefficients for the phonon and phason fields, respectively.

For the N-layered PQC plates, material properties can be written in the following form.

$$\begin{aligned} &C_{ij} = \sum_{n=1}^{N} C_{ij}^n I_{h_{n-1},h_n}, K_i = \sum_{n=1}^{N} K_i^n I_{h_{n-1},h_n}, R_i = \sum_{n=1}^{N} R_i^n I_{h_{n-1},h_n}, \rho = \sum_{n=1}^{N} \rho^n I_{h_{n-1},h_n}, \\ &e_{ij} = \sum_{n=1}^{N} e_{ij}^n I_{h_{n-1},h_n}, d_{ij} = \sum_{n=1}^{N} d_{ij}^n I_{h_{n-1},h_n}, \in_{ij} = \sum_{n=1}^{N} \in_{ij}^n I_{h_{n-1},h_n}, \end{aligned} \tag{5}$$

Where $C_{ij}^n, K_i^n, R_i^n, \rho^n, e_{ij}^n, d_{ij}^n, \in_{ij}^n$ are the material parameters of the Nth layer.

The displacements in the phonon and phason fields, and the electric potential can be written in the harmonic form.

$$u_x = U(z)e^{ikx-iwt}, u_z = W(z)e^{ikx-iwt}, w_z = \gamma(z)e^{ikx-iwt}, \phi = X(z)e^{ikx-iwt} \tag{6}$$

Where U(z), V(z), W(z), and γ(z) represent the amplitudes of the phonon and phason displacement components, respectively, and X(z) is the amplitude of the electric potential.

Substituting Eq. (2-6) into Eq. (1) yields the corresponding governing wave differential equation.

$$\begin{aligned} &-C_{11}k^2U + C_{55}U'' + (C_{13} + C_{55})ikW' + (R_1 + R_3)ik\gamma' + (e_{15} + e_{31})ikX' \\ &+C'_{55}U' + C'_{55}ikW + R'_3ik\gamma + e'_{15}ikX = -\rho\omega^2 U \end{aligned} \tag{7a}$$

$$\begin{aligned} &(C_{13} + C_{55})ikU' - C_{55}k^2W + C_{33}W'' - R_3k^2\gamma + R_2\gamma'' - e_{15}k^2X + e_{33}X'' \\ &+C'_{13}ikU + C'_{33}W' + R'_2\gamma' + e'_{33}X' = -\rho\omega^2 W \end{aligned} \tag{7b}$$

$$\begin{aligned} &(R_1 + R_3)ikU' - R_3k^2W + R_2W'' - K_2k^2\gamma + K_1\gamma'' - d_{15}k^2X + d_{33}X'' \\ &+R'_1ikU + R'_2W' + K'_1\gamma' + d'_{33}X' = -\rho\omega^2\gamma \end{aligned} \tag{7c}$$

$$\begin{aligned} &(e_{15} + e_{31})ikU' - e_{15}k^2W + e_{33}W'' - d_{15}k^2\gamma + d_{33}\gamma'' + \in_{11} k^2X \\ &- \in_{33} X'' + e'_{31}ikU + e'_{33}W' + d'_{33}\gamma' - \in'_{33} X' = 0 \end{aligned} \tag{7d}$$

Where the prime ' denotes the derivative with respect to the variable z.

To satisfy the continuity of stresses and displacements at the interlayer interfaces, we expand the phonon and phason displacement components and the electric potential of each layer into a series of Legendre polynomials.

For the first layer:

$$\begin{aligned} &u_a^1 = \sum_{m=0}^{\infty} p_m^{a,1} Q_m^1(z)\exp(ikx - i\omega t), w_z^1 = \sum_{m=0}^{\infty} r_m^1 Q_m^1(z)\exp(ikx - i\omega t), \\ &\phi^1 = \sum_{m=0}^{\infty} q_m^1 Q_m^1(z)\exp(ikx - i\omega t) \end{aligned} \tag{8}$$

Where $Q_m^1(z) = \sqrt{\frac{2m+1}{h_1 - h_0}} P_m\left(\frac{2z - (h_1 - h_0)}{h_1 - h_0}\right)$;

$$u_a^1(z=h_1)=u_a^{1,h_1}=\sum_{m=0}^{\infty}p_m^{a,1}Q_m^1(z=h_1)\exp(ikx-i\omega t),$$

$$w_z^1(z=h_1)=w_z^{1,h_1}=\sum_{m=0}^{\infty}r_m^1Q_m^1(z=h_1)\exp(ikx-i\omega t),$$

$$\phi^1(z=h_1)=\phi^{1,h_1}=\sum_{m=0}^{\infty}q_m^1Q_m^1(z=h_1)\exp(ikx-i\omega t),$$

Where $p_m^{a,n}(n=1,2)$, $r_m^n(n=1,2)$ and $q_m^n(n=1,2)$ are expansion coefficients, and P_m is the Legendre polynomials with order m.

For the second layer:

$$u_a^2=u_a^{1,h_1}+(z-h_1)\sum_{m=0}^{\infty}p_m^{a,2}Q_m^2(z)\exp(ikx-i\omega t),$$

$$w_z^2=w_z^{1,h_1}+(z-h_1)\sum_{m=0}^{\infty}r_m^2Q_m^2(z)\exp(ikx-i\omega t),\qquad(9)$$

$$\phi^2=\left(z/h_1\right)^2\phi^{1,h_1}+(z-h_1)\sum_{m=0}^{\infty}q_m^2Q_m^2(z)\exp(ikx-i\omega t),$$

Where $Q_m^2(z)=\sqrt{\frac{2m+1}{h_2-h_1}}P_m(\frac{2z-(h_2-h_1)}{h_2-h_1})$;

$$u_a^2(z=h_2)=u_a^{2,h_2}=u_a^{1,h_1}+(h_2-h_1)\sum_{m=0}^{\infty}p_m^{a,2}Q_m^2(z=h_2)\exp(ikx-i\omega t),$$

$$w_z^2(z=h_2)=w_z^{2,h_2}=w_z^{1,h_1}+(h_2-h_1)\sum_{m=0}^{\infty}r_m^2Q_m^2(z=h_2)\exp(ikx-i\omega t)$$

$$\phi^2(z=h_2)=\phi^{2,h_2}=\left(h_2/h_1\right)^2\phi^{1,h_1}+(h_2-h_1)\sum_{m=0}^{\infty}q_m^2Q_m^2(z=h_2)\exp(ikx-i\omega t)$$

For the N-th layer:

$$u_a^N=u_a^{N-1,h_{N-1}}+(z-h_{N-1})\sum_{m=0}^{\infty}p_m^{a,N}Q_m^N(z)\exp(ikx-i\omega t),$$

$$w_z^N=w_z^{N-1,h_{N-1}}+(z-h_{N-1})\sum_{m=0}^{\infty}r_m^NQ_m^N(z)\exp(ikx-i\omega t),\qquad(10)$$

$$\varphi^N=\left(z/h_{N-1}\right)^2\phi^{N-1,h_{N-1}}+(z-h_{N-1})\sum_{m=0}^{\infty}q_m^NQ_m^N(z)\exp(ikx-i\omega t),$$

With $Q_m^N(z)=\sqrt{\frac{2m+1}{h_N-h_{N-1}}}P_m(\frac{2z-(h_N-h_{N-1})}{h_N-h_{N-1}})$;

$$u_a^N(z=h_N)=u_a^{N,h_N}=u_a^{N-1,h_{N-1}}+(z-h_{N-1})\sum_{m=0}^{\infty}p_m^{a,N}Q_m^N(z=h_N)\exp(ikx-i\omega t),$$

$$w_z^N(z=h_N)=w_z^{N,h_N}=w_z^{N-1,h_{N-1}}+(z-h_{N-1})\sum_{m=0}^{\infty}r_m^NQ_m^N(z=h_N)\exp(ikx-i\omega t),$$

$$\phi^N(z=h_N)=\phi^{N,h_N}=\left(h_N/h_{N-1}\right)^2\phi_z^{N-1,h_{N-1}}+(h_N-h_{N-1})\sum_{m=0}^{\infty}r_m^NQ_m^N(z=h_N)\exp(ikx-i\omega t),$$

Substituting Eqs. (8)-(10) into Eq. (7), multiplying both sides by $Q_j^1(z),Q_j^2(z)\cdots Q_j^N(z)$, with j ranging from 0 to M, and then integrating with respect to z from 0 to hN, the following characteristic matrix is obtained by utilizing the orthogonality of Legendre polynomials.

$$\begin{bmatrix} {}^lA_{11}^{m,j} & {}^lA_{12}^{m,j} & {}^lA_{13}^{m,j} \\ {}^lA_{21}^{m,j} & {}^lA_{22}^{m,j} & {}^lA_{23}^{m,j} \\ {}^lA_{31}^{m,j} & {}^lA_{32}^{m,j} & {}^lA_{33}^{m,j} \end{bmatrix}\begin{Bmatrix} p_{m,j}^1 \\ p_{m,j}^2 \\ r_{m,j} \end{Bmatrix}=-\omega^2\begin{bmatrix} {}^lM_{m,j} & 0 & 0 \\ 0 & {}^lM_{m,j} & 0 \\ 0 & 0 & {}^lM_{m,j} \end{bmatrix}\begin{Bmatrix} p_{m,j}^1 \\ p_{m,j}^2 \\ r_{m,j} \end{Bmatrix}\qquad(11)$$

So far, the governing equations are thus reduced to a generalized eigenvalue problem to be solved. For the given k, the eigenvalues related to ω can be obtained.

3. Numerical Results

The PQC layered plate considered in this paper is assumed to be composed of two types of piezoelectric quasicrystal materials, abbreviated as PQC1 and PQC2. Their material constants are listed in Table 1.

Table 1. Material parameters of PQC1 and PQC2

Property	C_{11}	C_{12}	C_{13}	C_{22}	C_{23}	C_{33}	C_{44}	C_{55}
PQC1	23.433	5.741	6.663	23.433	6.663	23.222	7.019	7.019
PQC2	20	10	10	20	10	15	5	5
	C_{66}	ρ	R_1	R_2	R_3	K_1	K_2	e_{15}
PQC1	8.846	4.186	0.8846	0.8846	0.8846	122	24	11.6
PQC2	5	5.07	0.5	0.5	0.5	5	2	12.7
	e_{31}	e_{33}	e_{24}	d_{15}	d_{33}	d_{24}	$\in_{11}$	$\in_{33}$
PQC1	-4.4	18.6	11.6	1.16	1.86	1.16	5	10
PQC2	-5.2	15.1	12.7	1.27	1.51	1.27	6.5	5.6

Units: $C_{ij}(10^{10}N/m^2)$, $\rho(10^3kg/m^3)$, $R_i(10^9N/m^2)$, $K_i(10^9N/m^2)$, e_{ij}, $d_{ij}(C/m^2)$, $\in_{ij}(10^{-9}C^2/(N*m^2))$

First, the dispersion characteristics of Lamb waves in the PQC layered plates and the corresponding piezoelectric crystal (PC) plate are investigated. Figure 2 presents the phase velocity dispersion curves for the PQC plate with a PQC1/PQC2/PQC1 stacking sequence and thicknesses of 1mm/2mm/1mm. For the corresponding PC plate, $K_{ij} = R_{ij} = 0$ is set, while the other material constants remain unchanged. It can be seen that, similar to the single-layered and graded PQC plates, the first three modes have no cut-off frequency. They are A0, S0 and PL0 (the first phason mode) modes. The phonon modes exhibit similar wave characteristics to the elastic modes of the layered crystal plate, and the influence of the phonon-phason coupling effect on the phonon modes is very weak. Furthermore, the additional modes correspond to the phason modes owing to the phonon-phason coupling effect.

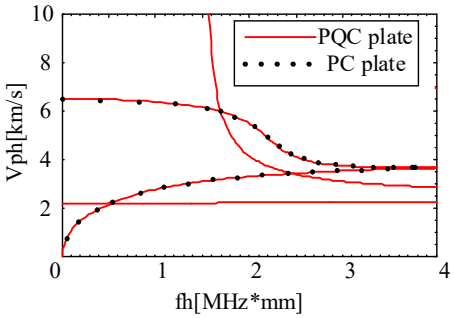

Figure 2. Phase velocity dispersion curves of Lamb waves in the PQC and PC layered plates

Subsequently, the effects of variation in layer thickness and stacking sequence on the wave characteristics of the PQC layered plates are investigated. Figure 3 illustrates the influence of variations in the layer thickness on the phase velocity dispersion curves. It can be observed that increasing the thickness of the PQC1 layer leads to an increase in the phase velocities of both the phonon and phason modes. This is because increasing the thickness of the PQC1 layer effectively increases its volume fraction. Furthermore, as can be seen from Table 1, the elastic parameters of both the phonon and phason fields in PQC1 are higher than those in PQC2. Although the density also changes, the increase in effective stiffness dominates the phase-velocity variation in the considered case. Consequently, this results in an overall increase in the corresponding phase velocities.

Then, the effect of the stacking sequence on the wave characteristics is analyzed. In this case, the thickness of the PQC2 layer is kept constant at 2 mm, while the thicknesses of the PQC1 layers are both set to 1 mm. The corresponding phase velocity dispersion curves are presented in Fig. 4. The stacking sequence has a significant influence on the phase velocities. Moreover, its impact varies notably between different phason and phonon modes. In summary, the desired wave characteristics can be achieved by tailoring the layer thickness and stacking sequence of the PQC layered plates.

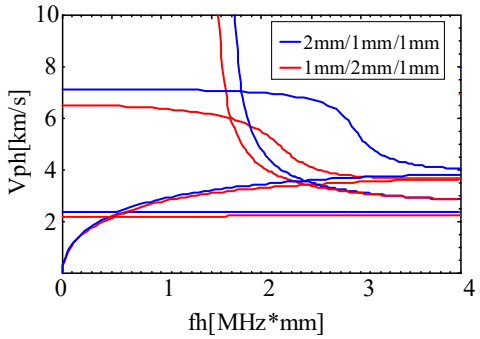

Figure 3. Phase velocity dispersion curves of the PQC1/PQC2/PQC1 plate with different layer thicknesses

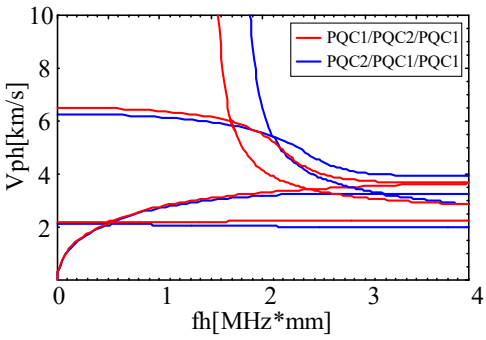

Figure 4. Phase velocity dispersion curves of the PQC layered plate with different stacking sequences

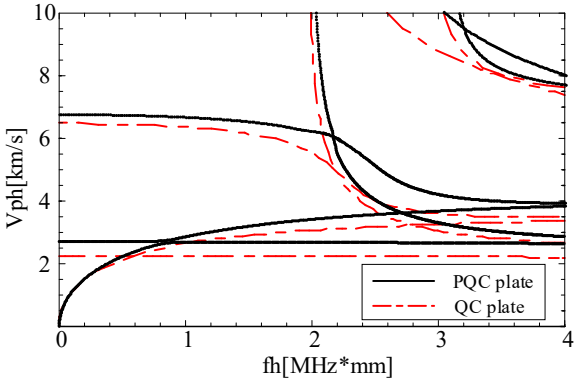

Figure 5. Phase velocity dispersion curves of the PQC and QC layered plates

Piezoelectric coupling is a key feature that strongly affects guided-wave propagation. Figure 5 presents the phase velocity dispersion curves for both the laminated

piezoelectric quasicrystal plate and the laminated quasicrystal plate. The structural parameters for the laminated piezoelectric quasicrystal plate are: PQC1/PQC2/PQC1 with thicknesses of 1mm/1mm/1mm, while those for the laminated quasicrystal plate are: QC1/QC2/QC1 with thicknesses of 1mm/1mm/1mm. For the laminated quasicrystal plate, the electric field material constants are set to zero, while all other material constants remain identical to those of the laminated piezoelectric quasicrystal plate. As can be seen from Fig. 5, the presence of the electric field increases the wave velocities of both the phason and phonon fields in the laminated piezoelectric quasicrystal plate, a characteristic that is consistent with crystal plates.

Subsequently, the effects of the outer and middle layers on the piezoelectric effect are discussed. For both phonon and phason modes, the piezoelectric effect is inversely proportional to the dielectric constant [19], that is, an increase in the dielectric constant leads to a decrease in the phase velocities of the phonon and phason modes. Assuming that all three layers of the PQC plates are composed of PQC1, the dielectric constants of the first and middle layers become $5\times \in_{ij}$, respectively. The corresponding phase velocity dispersion curves for the A0 mode are shown in Fig. 6. It can be observed that the phase velocity decreases as the dielectric constant increases. Furthermore, at low frequencies, the variation in the dielectric constant of the middle layer has a greater impact on the piezoelectric effect. Whereas at high frequencies, the variation in the dielectric constant of the first layer (surface layer) exerts a more significant influence.

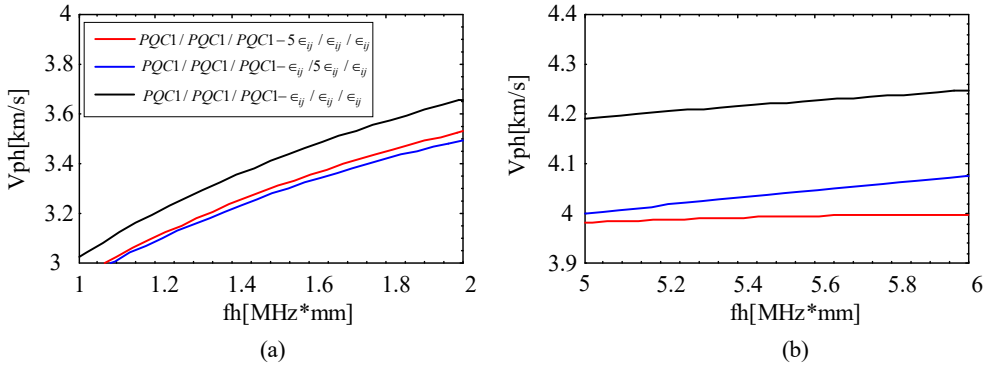

Figure 6. Phase velocity dispersion curves of the A0 mode for PQC layered plates with different dielectric constants

4. Conclusions

Using the Legendre polynomial method, the propagation characteristics of Lamb waves in one-dimensional hexagonal PQC layered plates are investigated. The effects of the piezoelectric effect, layer thickness, and stacking sequence on the wave characteristics are analyzed. Based on the theoretical results mentioned above, the following conclusions can be drawn:

The desired wave characteristics can be achieved by varying the layer thickness and stacking sequence of the PQC layered plate.

The piezoelectric effect increases the phase velocities of both the phason and phonon modes for Lamb waves.

At low frequencies, the variation in the dielectric constant of the middle layer has a greater impact on the piezoelectric effect, whereas at high frequencies, the variation in the dielectric constant of the surface layer exerts a more significant influence.

References

[1] Zhang, L., Guo, J., & Xing, Y. (2018). Bending deformation of multilayered one-dimensional hexagonal piezoelectric quasicrystal nanoplates with nonlocal effect. International Journal of Solids and Structures, 132, 278–302. https://doi.org/10.1016/j.ijsolstr.2017.10.013

[2] Singhal, A. (2025). Investigation of surface and interface effects of piezoelectric quasicrystal different models with propagation of shear horizontal and anti-plane shear horizontal wave. Acta Mechanica Sinica, 41(11), 524389. https://doi.org/10.1007/s10409-025-2438-8

[3] Li, Y., & Gao, Y. (2024). Three-dimensional axisymmetric analysis of annular one-dimensional hexagonal piezoelectric quasicrystal actuator/sensor with different configurations. Crystals, 14(11), 964. https://doi.org/10.3390/cryst14110964

[4] Lazar, M., & Agiasofitou, E. (2024). Three-dimensional and two-dimensional Green tensors of piezoelectric quasicrystals. Crystals, 14(10), 835. https://doi.org/10.3390/cryst14100835

[5] Feng, X., Zhang, L., Li, Y., et al. (2024). Electromechanical coupling characteristics of multilayered piezoelectric quasicrystal plates in an elastic medium. ZAMM-Journal of Applied Mathematics and Mechanics, 104(8), e202300464. https://doi.org/10.1002/zamm.202300464

[6] Qi, Y., & Rappe, A. M. (2021). Widespread negative longitudinal piezoelectric responses in ferroelectric crystals with layered structures. Physical Review Letters, 126(21), 217601. https://doi.org/10.1103/PhysRevLett.126.217601

[7] Gorgin, R., Luo, Y., & Wu, Z. (2020). Environmental and operational conditions effects on Lamb wave based structural health monitoring systems: A review. Ultrasonics, 105, 106114. https://doi.org/10.1016/j.ultras.2020.106114

[8] Tian, R., Yi, L., Nie, G., et al. (2025). Lamb waves in multilayered piezoelectric semiconductor plates. Applied Mathematics and Mechanics, 46(8), 1493–1510. https://doi.org/10.1007/s10483-025-2989-9

[9] Vashishth, A. K., & Bareja, U. (2025). Lamb wave propagation in a functionally graded porous piezoelectric material plate. Journal of the Brazilian Society of Mechanical Sciences and Engineering, 47(4), 199. https://doi.org/10.1007/s40440-025-04213-4

[10] Wang, X., Yu, J., Zhang, B., et al. (2025). Lamb waves in piezoelectric quasicrystal multi-layered nano-plates with imperfect interfaces. Composite Structures, 370, 119430. https://doi.org/10.1016/j.compstruct.2025.119430

[11] Shechtman, D. G., Blech, I. A., Gratias, D., et al. (1984). Metallic phase with long-range orientational order and no translational symmetry. Physical Review Letters, 53(20), 1951–1953. https://doi.org/10.1103/PhysRevLett.53.1951

[12] Lubensky, T. C., Ramaswamy, S., & Toner, J. (1985). Hydrodynamics of icosahedral quasicrystals. Physical Review

B, 32(11), 7444–7452. https://doi.org/10.1103/PhysRevB.32.7444

[13] Bak, P. (1985). Phenomenological theory of icosahedral incommensurate ("quasiperiodic") order in Mn-Al alloys. Physical Review Letters, 54(14), 1517–1520. https://doi.org/10.1103/PhysRevLett.54.1517

[14] Loboda, V., Sheveleva, A., Komarov, O., et al. (2025). A moving interface crack in 1D quasicrystal with piezoelectric effect. Mechanics of Advanced Materials and Structures. https://doi.org/10.1080/15376494.2025.2598864

[15] Su, X., Li, Z., Liang, F., et al. (2026). Free vibration symplectic analytical solutions of two-dimensional decagonal quasicrystal cylindrical shell panels. International Journal of Mechanics and Materials in Design, 22(1), 39. https://doi.org/10.1007/s10998-025-00892-1

[16] Fan, J., Li, L., & Chen, A. (2025). Postbuckling behavior of two-dimensional decagonal quasicrystal plates under biaxial compression. Mechanics of Advanced Materials and Structures, 32(8), 1579–1593. https://doi.org/10.1080/15376494.2024.2432162

[17] Feng, X., Zhang, L., Hu, Z., et al. (2022). Guided wave propagation in multilayered two-dimensional quasicrystal plates with imperfect interfaces. Acta Mechanica Solida Sinica, 35(4), 694–704. https://doi.org/10.1007/s10483-022-2868-8

[18] Zhang, B., Yu, J. G., & Zhang, X. M. (2020). Guided wave propagation in functionally graded one-dimensional hexagonal quasi-crystal plates. Journal of Mechanics, 36(6), 773–788. https://doi.org/10.1017/jmech.2020.43

[19] Zhang, B., Yu, J. G., Zhang, X. M., et al. (2021). Guided wave propagating in a 1-D hexagonal piezoelectric quasi-crystal plate. Acta Mechanica, 232(1), 135–151. https://doi.org/10.1007/s00707-020-02811-2

[20] Feng, X., Zhang, L., Li, Y., et al. (2023). On the propagation of plane waves in cubic quasicrystal plates with surface effects. Physics Letters A, 473, 128807. https://doi.org/10.1016/j.physleta.2023.128807